Supporting Information

Biochar as a Renewable Substitute for Carbon Black in Lithium-Ion Battery Electrodes

Seth Kane[a], Aksiin Storer[b], Wei Xu[b], Cecily Ryan[a], and Nicholas P. Stadie[b]*

[a] Department of Mechanical & Industrial Engineering, Montana State University, Bozeman, MT 59717, United States

[b] Department of Chemistry & Biochemistry, Montana State University, Bozeman, MT 59717, United States

*Email: nstadie@montana.edu

Number of pages: 14
Number of tables: 2
Number of figures: 9

S1. Greenhouse Gas Emissions Assessment Methods

An environmental impact assessment was performed with the goal of estimating the global warming potential of the production of biochar as a conductive additive in lithium-ion batteries (LIBs) compared to commercially obtained carbon black. To this end, no environmental impact categories other than global warming potential were considered. We hypothesized that biochar would reduce the global warming potential associated with the production of a conductive additive relative to carbon black. This cradle-to-gate estimation was made with a functional unit of 1 kg conductive additive, comparing the production of biochar from lignin to the production of Vulcan XC-72R carbon black from petroleum (**Figure S1**).

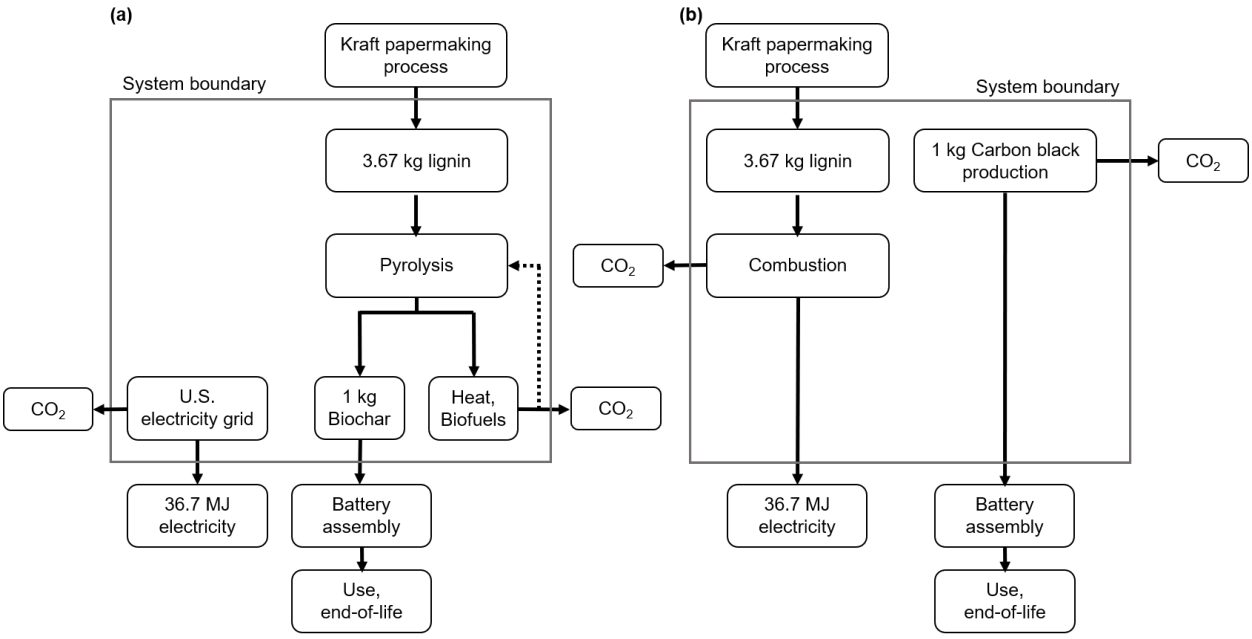

Figure S1. System boundaries for the greenhouse gas emissions assessment performed to compare the global warming potential of the production of (a) biochar and (b) carbon black.

This estimation is made with the following assumptions: (1) that all carbon in the gas and liquid pyrolysis products is completely combusted to form CO_2, (2) that otherwise all carbon in the lignin would be completely combusted for energy, and (3) that lignin is a waste byproduct, and therefore all emissions associated with biomass production can be attributed to the other products of the kraft process. In the comparison scenario, 3.67 kg of lignin is combusted to generate 36.15 MJ of energy[S1] was converted into biochar in the primary scenario. This combustion generates 36.15 MJ of energy; to avoid allocation, this is accounted for in the primary scenario by the addition of the production of energy at the 2020 U.S. electricity grid average.[S2] It is assumed that the pyrolysis process is net energy neutral: i.e., that the heat generated from exothermic pyrolytic reactions and combustion of the gas and liquid products is used to heat the pyrolysis process.[S3–5] The fact that biochar pyrolysis produces surplus energy has been established and demonstrated to produce lower temperature biochars, and it is assumed herein that this also holds true at higher temperatures (no data for pyrolysis above 900 ºC was found in the literature).

The battery production, application, and end-of-life phases of the material were outside the scope of this estimation. However, given the similar performance of biochar compared to carbon black as a conductive additive, it is a reasonable assumption that the substitution of carbon black with biochar would have minimal impact on these aspects of the assessment.

S2. Further Materials Characterization

In addition to the XRD patterns and Raman spectra presented in the main text, all conductive additive materials were characterized by EDX spectroscopy to determine the chemical composition (**Figure S2a**). All of the materials were found to be mainly carbon (89-99 at. %), with some oxygen (0.7-7 at. %) and sulfur (0-2 at. %) also present. Biochar shows higher oxygen and sulfur content than carbon black, in addition to sodium. The sodium content in biochar can be attributed to the presence of sodium sulfate (Na_2SO_4) as confirmed by XRD and FTIR (**Figures S2b-S2c**) and is significantly reduced by washing in copious water; hence, the washing procedure used herein is a simple and effective method to remove sodium sulfate.

All three conductive additive materials were also assessed in terms of particle size using optical methods (**Figure S2d**). Biochar, XC-72, and Super P all show similar particle size distributions, with biochar having a slightly smaller median particle size than the agglomerates present in both carbon blacks, and with all three materials having a median particle size of ~10 μm.

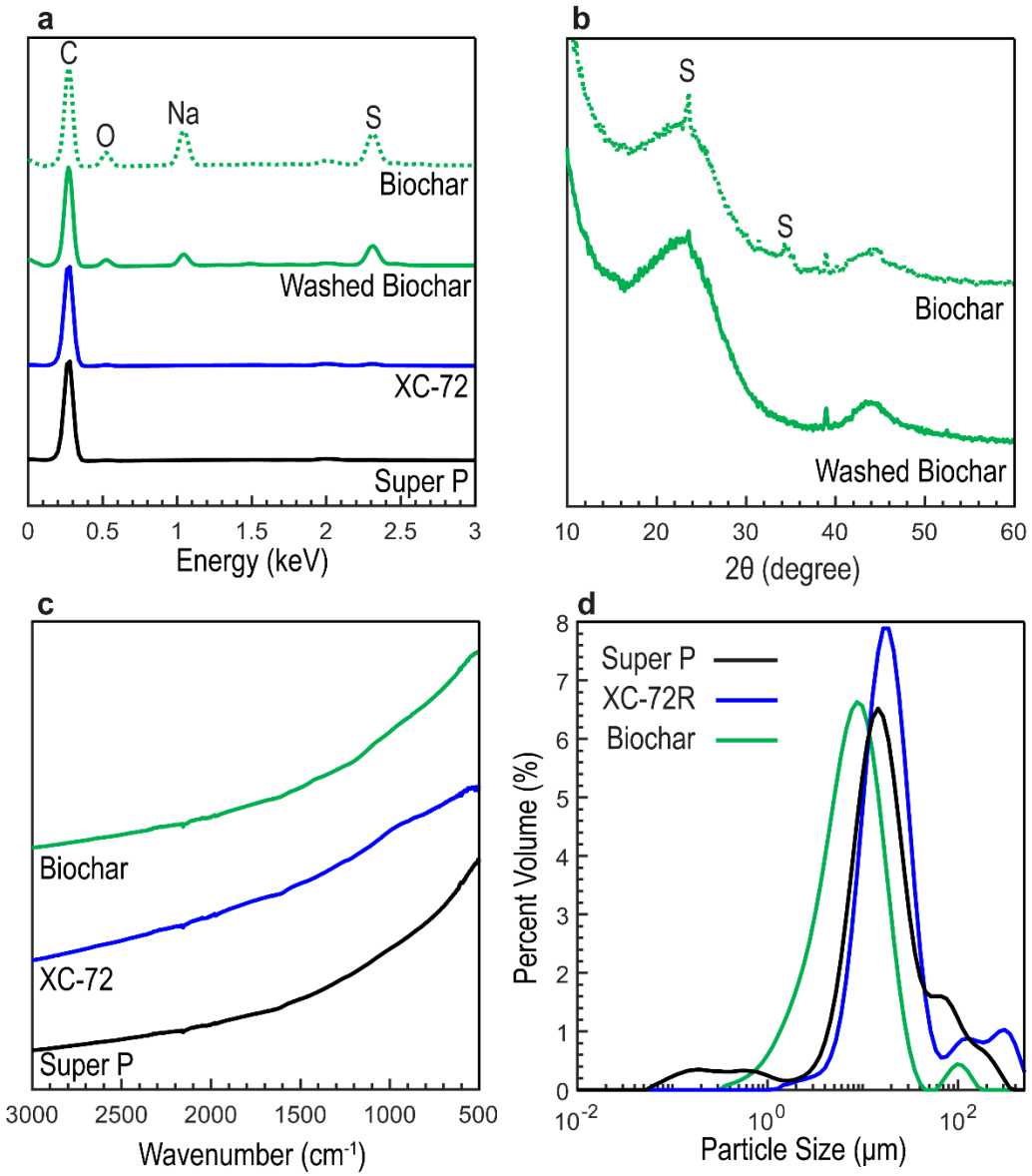

Figure S2. Further materials characterization of Super P, Vulcan XC-72, and biochar (before and after washing with deionized water). (a) EDX spectra, (b) XRD patterns, (c) FTIR spectra, and (d) optical particle size distributions.

S3. Further Active Materials Electrochemical Characterization

For each set of electrochemical results presented in Figures 2-3 in the main text, at least three cells were fabricated to ensure reproducibility of the results. In some cases, many more cells and electrodes were tested. All of the replicate tests showed high consistency from cell to cell, as shown in **Figures S3-S4**. In all cases presented in the main text, the middle cell (or the cell nearest the mean) of any given series of replicates was used.

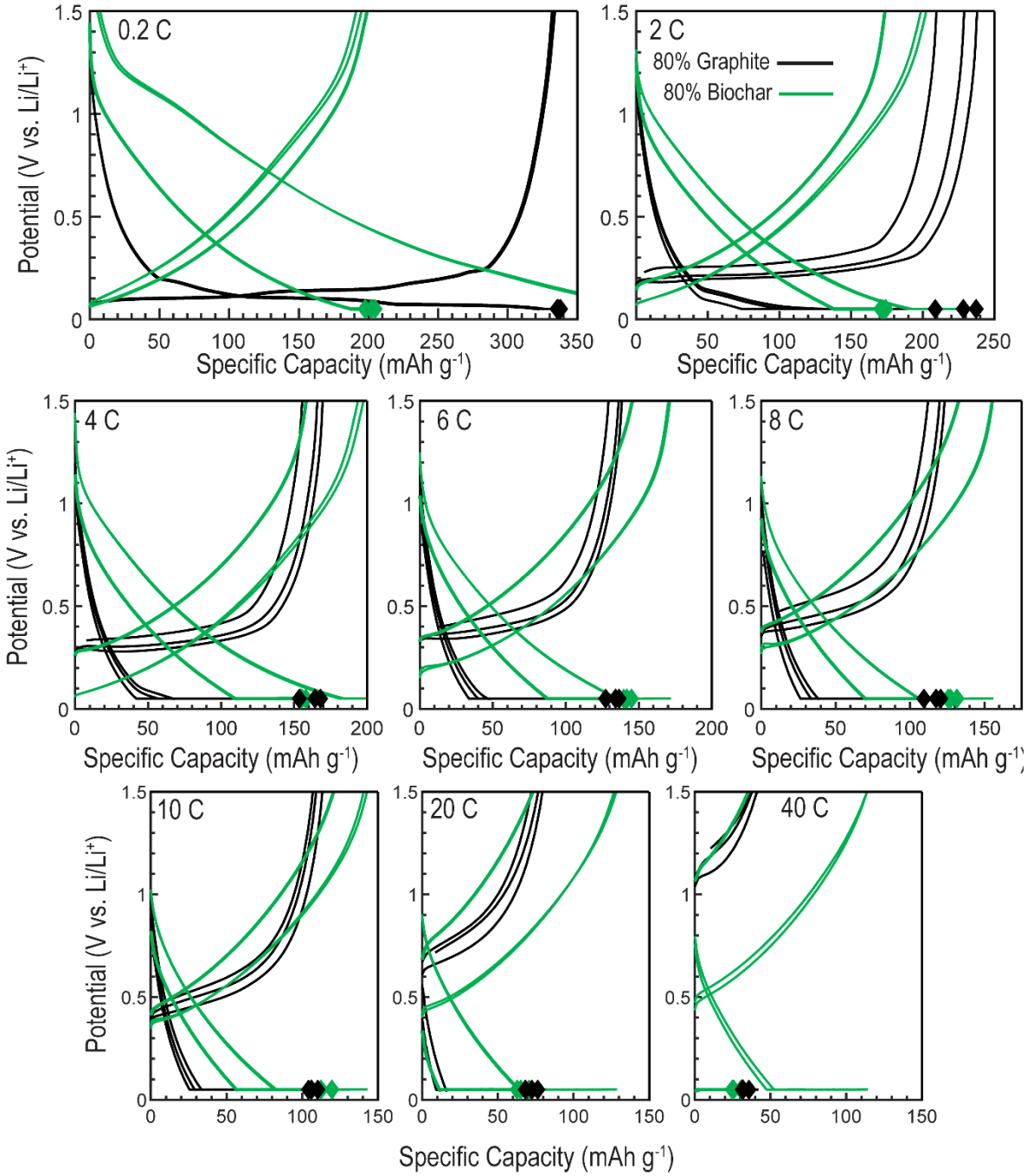

Figure S3. Replicate electrochemical characterization of electrodes containing 80% biochar or graphite as the active material, between 0.2 C (top left) and 40 C (bottom right).

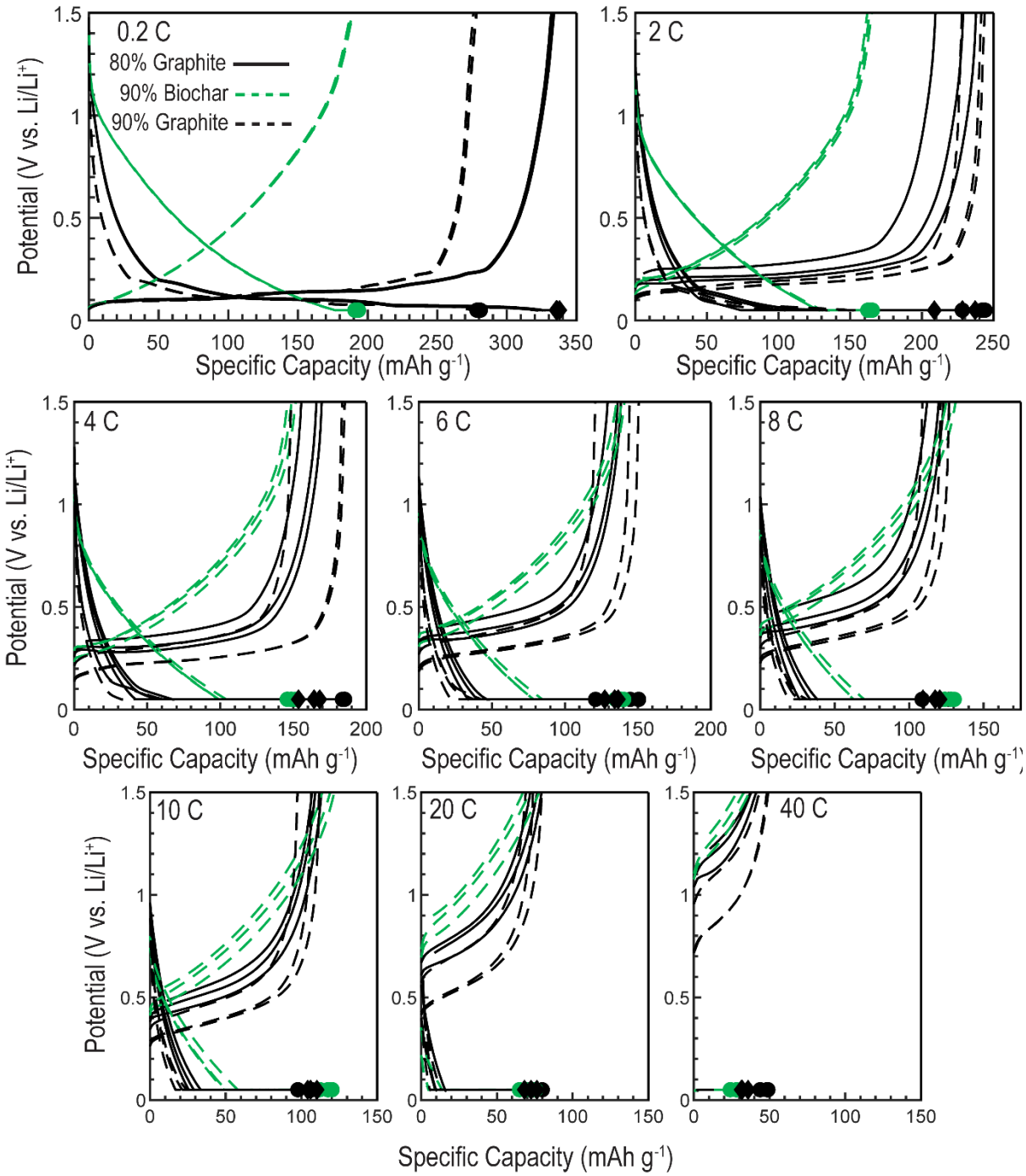

Figure S4. Replicate electrochemical characterization of electrodes containing 90% biochar and graphite (no conductive additive) compared to electrodes containing 80% graphite and 10% Super P between 0.2 C (top left) and 40 C (bottom right).

Table S1. Specific capacity and Coulombic efficiency for electrodes with 80% or 90% biochar (BioC) or artificial graphite (AG) as the active material. All reported values are means of three replicates and all errors are one standard deviation.

Rate (C)	**0.2**	**2**	**4**	**6**	**8**	**10**	**20**	**40**	**20**	**10**	**8**	**6**	**4**	**2**
Cycle Number	**5**	**15**	**25**	**35**	**45**	**55**	**65**	**75**	**85**	**95**	**105**	**115**	**125**	**135**
Specific Capacity (mAh g^{-1})														
80% BioC	201.6 ± 2.9	172.4 ± 1.4	156.6 ± 1.5	143.3 ± 2.1	129.6 ± 2.5	116.7 ± 3.3	69.7 ± 3.4	32.6 ± 2.9	67.0 ± 3.9	105.2 ± 4.0	120.6 ± 6.1	138.8 ± 5.7	159.3 ± 2.0	173.5 ± 1.3
80% AG	336.5 ± 1.0	225.8 ± 11.9	163.9 ± 5.9	135.1 ± 2.9	118.8 ± 4.7	110.2 ± 2.6	76.9 ± 3.1	39.7 ± 1.8	74.6 ± 1.8	108.0 ± 1.1	121.4 ± 1.8	139.3 ± 2.7	167.7 ± 9.5	209.2 ± 20.0
90% BioC	192.6 ± 1.2	164.0 ± 1.3	149.2 ± 2.2	138.8 ± 2.3	129.0 ± 2.5	118.7 ± 3.3	73.5 ± 4.5	33.5 ± 3.2	69.5 ± 5.0	108.2 ± 5.6	121.1 ± 7.4	137.1 ± 5.8	152.3 ± 1.8	164.8 ± 0.7
90% AG	280.7 ± 1.0	239.1 ± 6.6	173.1 ± 17.0	138.9 ± 13.3	118.7 ± 8.6	105.6 ± 5.9	74.8 ± 4.3	47.7 ± 2.4	74.5 ± 2.9	104.0 ± 4.0	115.3 ± 4.1	132.7 ± 3.5	162.3 ± 3.5	218.6 ± 5.3
Coulombic Efficiency (%)														
80% BioC	97.6 ± 0.4	99.7 ± 0.0	99.8 ± 0.1	99.8 ± 0.0	99.7 ± 0.0	99.6 ± 0.1	98.5 ± 0.4	98.8 ± 0.4	99.4 ± 0.2	99.4 ± 0.2	99.4 ± 0.3	99.8 ± 0.1	99.8 ± 0.0	99.8 ± 0.1
80% AG	98.9 ± 0.0	99.8 ± 0.0	99.8 ± 0.0	99.7 ± 0.1	99.7 ± 0.0	99.7 ± 0.1	99.2 ± 0.1	98.5 ± 0.2	99.4 ± 0.1	99.6 ± 0.0	99.7 ± 0.0	99.8 ± 0.0	99.9 ± 0.1	99.9 ± 0.0
90% BioC	98.1 ± 0.3	99.7 ± 0.0	99.8 ± 0.0	99.8 ± 0.0	99.7 ± 0.0	99.6 ± 0.0	98.5 ± 0.0	98.8 ± 0.0	99.2 ± 0.0	99.3 ± 0.0	99.7 ± 0.0	99.8 ± 0.0	99.8 ± 0.0	99.8 ± 0.0
90% AG	98.9 ± 0.1	99.9 ± 0.0	99.9 ± 0.0	99.9 ± 0.1	99.7 ± 0.1	99.8 ± 0.0	99.3 ± 0.1	99.8 ± 0.3	99.2 ± 0.2	99.8 ± 0.1	99.8 ± 0.1	99.9 ± 0.01	100.0 ± 0.1	99.9 ± 0.0

S4. Further Anode Additive Characterization

As a conductive additive for LIB anodes (e.g., graphite), further electrochemical characterization of biochar, Super P, and Vulcan XC-72 was carried out to ensure reproducibility across multiple cells (**Figure S5**) and to compare electrical conductivity of the prepared electrodes (**Figure S6**).

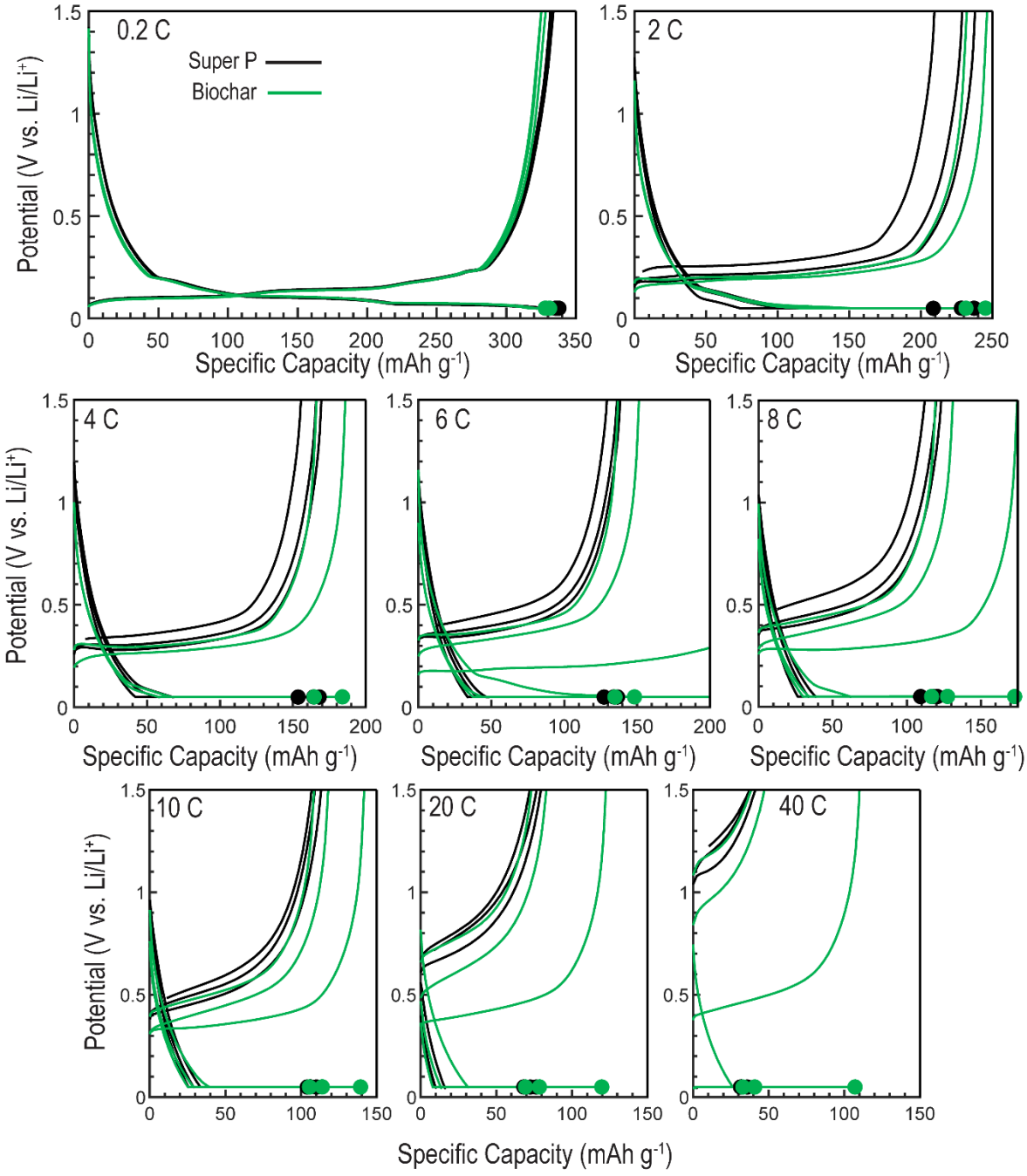

Figure S5. Replicate electrochemical characterization of electrodes containing biochar or Super P as the conductive additive (10%), between 0.2 C (top left) and 40 C (bottom right).

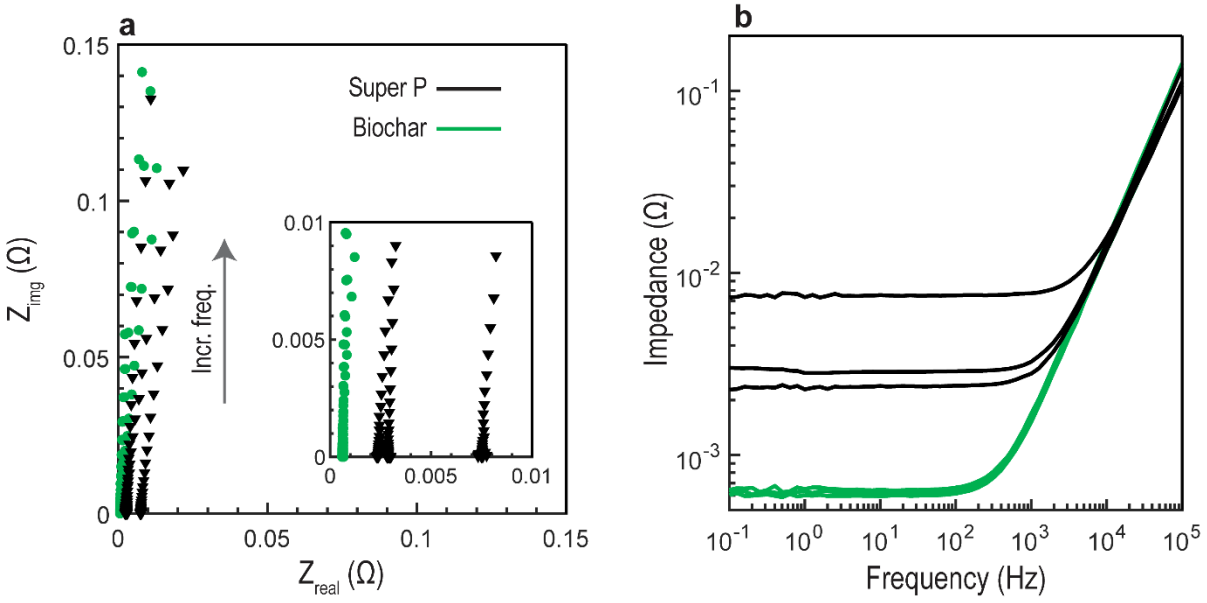

Figure S6. Replicate EIS spectra of electrodes containing biochar or Super P as the conductive additive (10%): (a) Nyquist plot, with inset highlighting the low impedance region and (b) Bode plot.

Electrical impedance spectroscopy (EIS) of ex situ, never cycled electrodes containing either biochar or Super P as the conductive additive (10%). This result confirms that the slight increase in electrical conductivity biochar compared to carbon black, as shown in **Figure 1a** in the main text, translates to increased electrical conductivity in the anode. Biochar is observed to exhibit higher average electrical conductivity than Super P; for ex situ anodes prepared with biochar or Super P as the conductive additive, Super P shows an average impedance (0.004 Ω) approximately one order of magnitude higher than that of anodes prepared with biochar (0.0006 Ω) at frequencies below 100 Hz. The impedance behavior for both anodes is largely resistive, with inductive behavior seen at higher frequencies (>1000 Hz), which is attributable to experimental measurement conditions. [S6]

Table S2. Specific capacity and Coulombic efficiency for electrodes with biochar or Super P as the conductive additive. All reported values are means of three replicates and all errors are one standard deviation.

Rate (C)	**0.2**	**2**	**4**	**6**	**8**	**10**	**20**	**40**	**20**	**10**	**8**	**6**	**4**	**2**
Cycle Number	**5**	**15**	**25**	**35**	**45**	**55**	**65**	**75**	**85**	**95**	**105**	**115**	**125**	**135**
							Specific Capacity (mAh g^{-1})							
Biochar	329.2 ± 1.4	240.5 ± 6.0	175.8 ± 8.1	143.7 ± 5.9	124.6 ± 4.9	112.6 ± 4.2	77.4 ± 4.5	43.1 ± 4.1	78.7 ± 4.0	112.1 ± 6.0	122.8 ± 3.6	140.7 ± 2.7	172.6 ± 9.3	237.3 ± 15.6
Super P	336.5 ± 1.0	225.8 ± 11.9	163.9 ± 5.9	135.1 ± 3.9	118.8 ± 4.7	110.2 ± 2.6	76.9 ± 3.1	39.7 ± 1.8	74.6 ± 1.8	108.0 ± 1.1	121.4 ± 1.8	139.3 ± 2.7	167.7 ± 9.5	209.2 ± 20.0
							Coulombic Efficiency (%)							
Biochar	99.1 ± 0.0	99.9 ± 0.0	99.9 ± 0.0	99.9 ± 0.1	99.8 ± 0.0	99.7 ± 0.0	99.1 ± 0.1	97.4 ± 0.9	99.3 ± 0.2	00.8 ± 0.1	100 ± 0.0	100 ± 0.1	99.9 ± 0.0	99.9 ± 0.0
Super P	98.9 ± 0.0	99.8 ± 0.0	99.8 ± 0.0	99.7 ± 0.1	99.7 ± 0.0	99.7 ± 0.1	99.2 ± 0.1	98.5 ± 0.2	99.4 ± 0.1	99.6 ± 0.0	99.7 ± 0.0	99.8 ± 0.0	99.9 ± 0.1	99.9 ± 0.0

S5. Cathode Additive Characterization

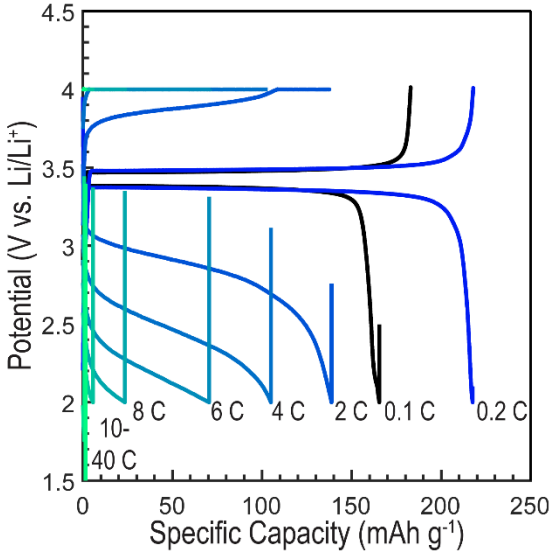

Figure S7. Electrochemical characterization of LFP cathodes containing carbon black as the conductive additive from 0.1 C to 40 C. LFP-based electrodes containing biochar as a conductive additive could not be successfully cycled.

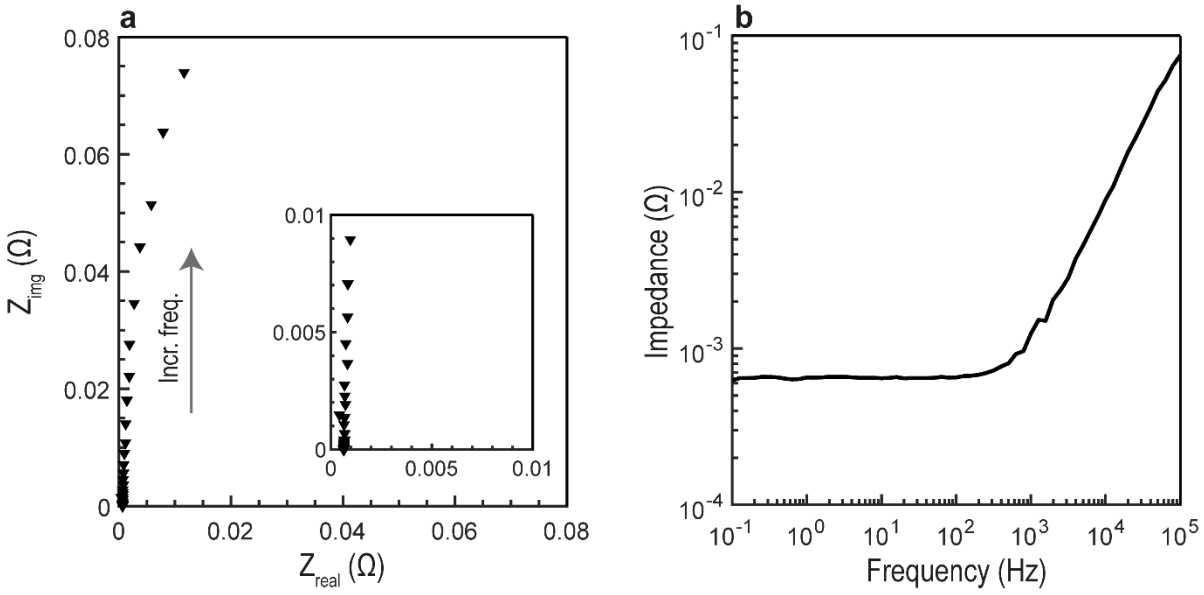

Figure S8. EIS spectra of an LFP-based cathode with Super P as the conductive additive: (a) Nyquist plot, with detailed inset, and (b) Bode plot. Electrodes with biochar as the conductive additive exhibited an impedance above the upper limit of the instrument (>1.5 GΩ).

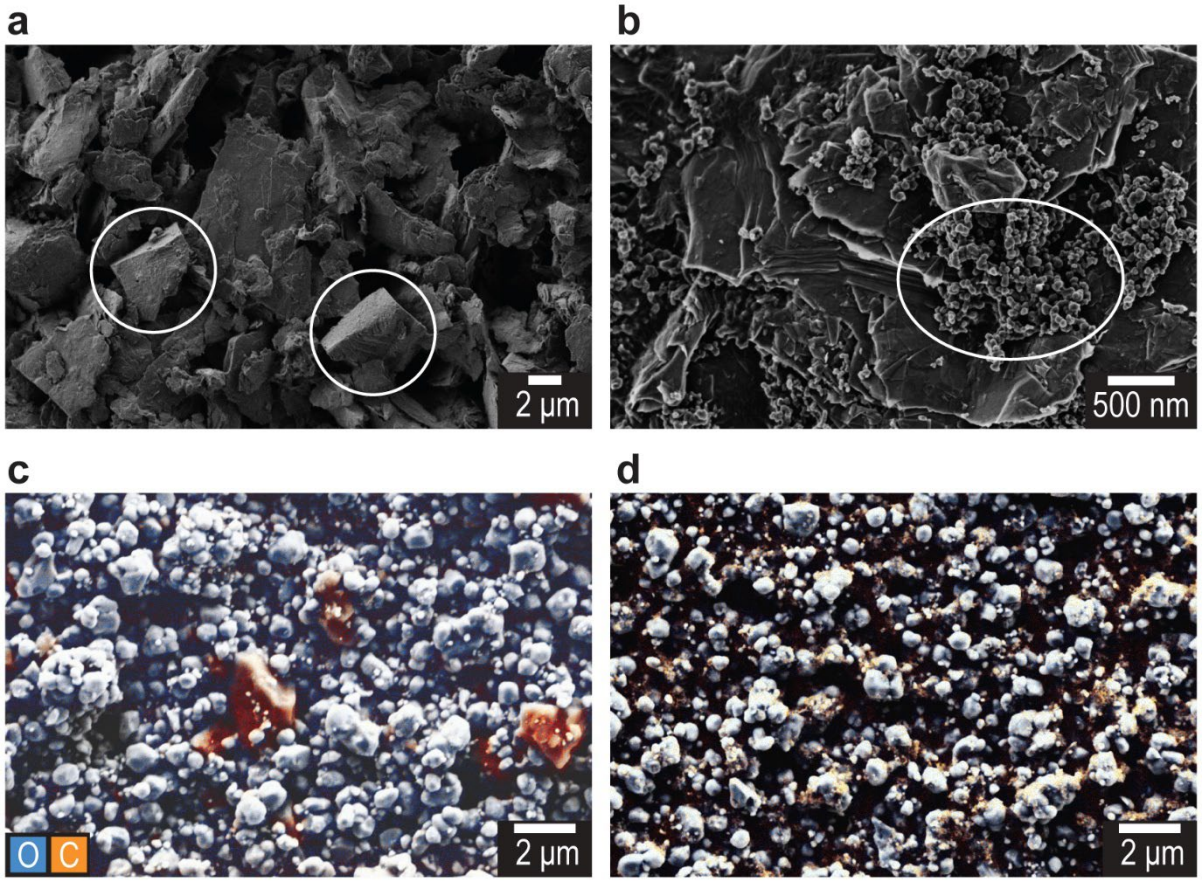

Figure S9. SEM micrographs of as-prepared graphite-based electrodes with (a,c) biochar and (b,d) Super P as the conductive additive (at 10,500× and 83,000× magnification, respectively). Biochar and Super P are shown in white circles. Elemental maps of showing carbon and oxygen distribution are shown in orange and blue, respectively, as measured by EDX; these can be used to differentiate between conductive additive and active LFP, respectively. In both electrodes, fluorine was found to be evenly distributed, indicating minimal localization of the PVDF binder.

S6. Supporting References

(S1) Bernier, E.; Lavigne, C.; Robidoux, P. Y. Life Cycle Assessment of Kraft Lignin for Polymer Applications. *International Journal of Life Cycle Assessment* **2013**, *18* (2), 520–528. https://doi.org/10.1007/S11367-012-0503-Y/FIGURES/3.

(S2) U.S. Energy Information Administration. Electricity Data https://www.eia.gov/electricity/data.php (accessed 2021 -12 -29).

(S3) Koderra, Y.; Kaiho, M. Model Calculation of Heat Balance of Wood Pyrolysis. *Journal of the Japan Institute of Energy* **2016**, *95* (10), 881–889. https://doi.org/10.3775/JIE.95.881.

(S4) Xu, R.; Ferrante, L.; Hall, K.; Briens, C.; Berruti, F. Thermal Self-Sustainability of Biochar Production by Pyrolysis. *Journal of Analytical and Applied Pyrolysis* **2011**, *91* (1), 55–66. https://doi.org/10.1016/J.JAAP.2011.01.001.

(S5) Peters, J. F.; Iribarren, D.; Dufour, J. Biomass Pyrolysis for Biochar or Energy Applications? A Life Cycle Assessment. *Environmental Science and Technology* **2015**, *49* (8), 5195–5202. https://doi.org/10.1021/ES5060786/SUPPL_FILE/ES5060786_SI_001.PDF.

(S6) Kane, S.; Warnat, S.; Ryan, C. Improvements in Methods for Measuring the Volume Conductivity of Electrically Conductive Carbon Powders. *Advanced Powder Technology* **2021**, *32* (3), 702–709. https://doi.org/10.1016/J.APT.2021.01.016.